Excitation effect of *d* electrons on the electronic energy loss of energetic protons colliding with a Zn atom

Xu-Dong Zhao,[1] Fei Mao,[1,*] Sheng-An Tang,[1] Cong-Zhang Gao,[2] Feng Wang,[3] and Feng-Shou Zhang[4]

[1]*School of Nuclear Science and Technology, University of South China, Hengyang 421001, China*

[2]*Institute of Applied Physics and Computational Mathematics, Beijing 100094, China*

[3]*School of Physics, Beijing Institute of Technology, Beijing 100081, China*

[4]*The Key Laboratory of Beam Technology and Material Modification of Ministry of Education, College of Nuclear Science and Technology, Beijing Normal University, Beijing 100875, China*

(Received 16 February 2020; accepted 20 May 2020; published 11 June 2020)

By using a nonequilibrium approach based on real-time time-dependent density-functional theory combined with molecular dynamics simulations, the effects of *d*-electron excitation on the electronic energy loss of energetic protons colliding with atomic zinc target are studied. The results show that the semicore electrons play a crucial role in the electronic energy loss in an extended energy range. In the low-energy regime, the electronic energy loss displays the threshold effect before it is proportional to velocity, which is explained by the quantization of the energy levels of zinc atom, and the charge transfer contributes greatly to the electronic energy loss, especially at 0.1 a.u. In addition, due to the electron resonance excitation, the number of excited electrons and charge transfer is significantly increased at the velocity thresholds for electron excitation. In the high-energy regime, the electronic energy loss is greatly enhanced as the the impact parameter decreases, which is ascribed to the excitation of 3*d* electrons. We also calculated the stopping cross section for energetic protons colliding with atomic zinc, which is in a good agreement with the experimental values in both low- and high-velocity regimes.

DOI: 10.1103/PhysRevA.101.062705

I. INTRODUCTION

The study of the interactions between charged particles and materials not only plays an important role in understanding the physical mechanism of energy deposition by ion irradiation [1] but also makes great sense for nuclear safety, nuclear engineering and ion beam implantation modification [2]. Over the past few decades, a great deal of research has been carried out to study the mechanism of ion-matter interaction [3–7]. The energy dissipated by ions per unit path length in material is formally known as stopping power, the energy loss transferred to the host electrons is electronic stopping power, and the energy losses due to collision with the nuclei of the target is nuclear stopping power. The electronic stopping power has been studied continuously for many years, but there still leaves a lot of problems. Meanwhile, many models and theories have been proposed to understand the physical mechanisms of electron excitation, such as free electron gas model [8] and time-dependent density-functional theory (TDDFT) [9,10].

From the view of energy transfer, the electronic energy loss of ions colliding with atoms is a nonequilibrium and nonadiabatic process. TDDFT is a nonperturbative method which can be used to treat the electronic excitation effects under ion irradiation conditions [11,12]. TDDFT converts full many-electron time-dependent Schrödinger equation into a set of time-dependent one-particle Kohn-Sham equations, which directly produces a time-dependent single-particle density system. It significantly reduces the computational cost compared to conventional quantum mechanical methods and can be used to study many-electron systems. In recent years, real-time TDDFT (RT-TDDFT) has been widely used in the study of ion-solid interactions. Quashie *et al.* [13] showed the difference of electron excitation under channeling and off-channeling conditions when the protons are traversing in metal Cu. Lim *et al.* [14] reported a "elevator" state created by the addition of the channeling ion, which lifts the electrons from valence band maximum to conduction band minimum and causes a structured nonzero electronic stopping power in the prethreshold regime below 60 eV ($v < 0.2$ Å fs^{-1}) for self-irradiated Si ions. Recently, Quashie *et al.* [15] studied the self-interaction effect of different exchange and correlation (XC) functionals, which leads to deviations on the nonadiabatic forces with respect to the non-self-interacting case when the impact parameters are large. The agreement between the simulation results and the experimental data convinces that the RT-TDDFT model can be used to study the ion-solid interactions, and to explore the fundamental physical mechanism of electronic energy loss.

The role played by the core electrons in the electronic stopping power has been studied for many decades, both experimentally [16–18] and via computer simulations [19,20]. When a charged particle collides with target atoms, the dominant channel for energy losses is the electronic stopping in the high-energy region. The effects of core electrons of both projectile and target atoms on the electronic stopping power are discussed by Yao *et al.* [21] and Ullah *et al.* [22] within

*Corresponding author: maofei@mail.bnu.edu.cn

RT-TDDFT, the results show that the presence of core electrons provides an additional channel for energy loss, and affects the excitation of valence electrons. Experimentally, Gobel *et al.* [23] displayed two distinct regimes of the velocity proportional stopping for low-energy H^+ and He^{2+} ions traveling through bulk Zn and In, in which the onset of the transition regime, the kink velocity, is attributed to the contribution of *d* electron excitations of the target atoms.

Investigation of the ion-atom collisions also makes sense to understand the effects of core electrons on the electronic energy loss. In recent years, many theoretical studies on ion-atom and ion-molecule collisions have been reported. Castro *et al.* [24] simulated the scattering of protons with the Li_4 cluster, the results showed that the reaction channels are dependent on the incidence angle of the protons, and the charge transfer is a critical channel for the electronic energy loss in ion-atom collisions in the low-energy regime. Avendaño-Franco *et al.* [25] studied the charge transfer in the collision between the proton and helium atom, in which the evolution of charge density of ion-atom system during collision is described in detail by space partition monitoring. Wang *et al.* [26] calculated the charges captured by the protons after colliding with Ar atoms, the results are in good agreement with the experimental data, and divided the contributions from different electron orbitals to charge transfer.

For the end of understanding the role played by *d* electrons in the electronic stopping power of bulk zinc, it is necessary to study the contribution of *d* electrons excitation to the electronic energy loss of protons colliding with zinc atoms. In this article, we investigated the effects of *d* electrons excitation on the electronic energy loss when protons colliding with zinc atoms.

II. METHOD AND COMPUTATIONAL DETAILS

The TDDFT simulations are performed to study the effects of 3*d*-electron excitation on the electronic energy loss of protons colliding with atomic zinc by using OCTOPUS code [27,28]. In this theoretical framework, TDDFT calculations for electrons are combined with molecular dynamics simulations for ions in real time and real space. This method allows *ab initio* molecular dynamics simulation for excited electronic states. In Ehrenfest MD, transitions between electronic adiabatic states are considered, and it couples the populations of the adiabatic states to the nuclei trajectories [29]. It opens a way to study the electron transfer between the ions and the target electrons in the collisions [25]. The adiabatic local density approximation with Perdew-Wang analytic representation [30] for the XC functional is employed in the time-evolving simulation. The Verlet algorithm is used for the integration of ionic motion equations, and the approximated enforced time reversal symmetry method [31] is adopted to propagate the electronic wave functions. The interactions between valence electrons and ionic cores are described by the norm-conserving Troullier-Martins pseudopotential [32]. In this research, there are two pseudopotential models are built to represent Zn atom, one contains only 4*s* electrons in the valence electronic configuration which is referred to model A ($[Ar3d^{10}]4s^2$) for the convenience described below, the other one includes both 4*s* and 3*d* electrons which is referred to model B ($[Ar]3d^{10}4s^2$). There are 2 electrons in 4*s* state and 12 electrons in 3*d*+4*s* states considered in the pesudopotentials for model A and model B, respectively.

In the simulation, a rectangular simulation box with dimensions of 12 Å × 12 Å × 20 Å is employed. The external potential, electron density and Kohn-Sham orbitals are discretized in a set of mesh grid points with uniform spacing of 0.16 Å, which has been proven to get well converged results, along all three spatial coordinates in real space in the simulation cell. Before the time-dependent calculations, the zinc atom is located at the center of the simulation box, all the valence electrons of the target Zn atom are in their ground states. The initial ground-state Kohn-Sham orbitals are set up by diagonalization of the time-independent KS Hamiltonian for the atomic zinc, and the initial wave function is constructed by linear combination of atomic orbitals method.

The proton is originally located outside the simulation box, and the separation between the ion and the atom along the *z* axis is 21 Å. In the case of protons colliding with bulk Zn along the center of the channel in *c*-axis direction, the impact parameter (b) between the ions and closest zinc atom lines is 0.77 Å. The initial velocity is parallel to the *z* axis and $b = 0.77$ Å at the beginning of the time-dependent propagation. In order to quantify the effects of impact parameter on *d* electrons excitation, another set of simulations with $b = 1$ Å are also performed. In the collisions, the target electrons can be ionized and go asymptotically to infinity. In order to avoid artificial reflections of the electronic wave functions from the boundaries in the collisions, the complex absorbing potential is added at the boundaries of the simulation box [33], which can absorbs the outgoing waves in the time-dependent simulations.

To keep the total energy conservation for different incident velocities ranging from 0.1 a.u. to 4.0 a.u., we choose different Δt so that $\Delta t \times v \sim 3.4559 \times 10^{-3}$ Å except for the case of 0.1 a.u., in which a smaller timestep is required. The nucleus of the target atom is fixed at the initial position during the collision processes, so that the nuclear stopping can be excluded from the energy loss in this way, then the kinetic energy losses of the protons are totally transferred to the electronic subsystem of Zn atom, which is considered as the electronic energy loss in this study.

In order to obtain the contribution of *d*-electron excitation to the electronic energy loss, the time-dependent occupation number of electrons $n_{oc}(t)$ in 3*d* and 4*s* states in a nonadiabatic simulation can be obtained by projecting the time-dependent Kohn-Sham wave functions $|\psi_{n'}(t)\rangle$ on to the ground-state wave function $|\phi_n\rangle$:

$$n_{\rm oc}(t) = \sum_{nn'} |\langle\phi_n|\psi_{n'}(t)\rangle|^2. \tag{1}$$

Meanwhile, the number of excited electrons can be calculated by the following formula [34]:

$$n_{\rm ex}(t) = \sum_{nn'} [\delta_{nn'} - |\langle\phi_n|\psi_{n'}(t)\rangle|^2], \tag{2}$$

$n_{\rm ex}$ is the number of excited electrons from the ground states.

The advantage of the real-space grid method is that spatial coordination can be performed, so that the projectile and

the target atom can be separated, and the amount of charge transfer can be calculated after collision [26]. The separation between the proton and zinc atom is long enough in the simulation box after the collisions. Then the simulation box can be divided into two regions, the integration volume (Ω) around the projectile, and its complement. We calculated the charge transfer by integrating the charge density around the protons after colliding with zinc atoms,

$$e_{\text{transfer}}(t) = \int_{\Omega} \rho(\vec{r}(t))dV, \tag{3}$$

in which

$$\Omega = \frac{4\pi r_c^3}{3}, \tag{4}$$

where r_c is the integration radius of the charge density distribution of the outgoing proton, at which the charge density approaches zero. The integration radius $r_c = 2$ Å is used in the study.

By calculating the electronic energy loss under different impact parameters, we obtained the stopping cross section (SCS) for protons colliding with atomic zinc:

$$S(v) = 2\pi \int_0^{\infty} \Delta E(b) b db, \tag{5}$$

where b is the impact parameter, and ΔE represents the electronic energy loss which is defined by $\Delta E = E_i - E_f$, where E_i and E_f are the initial and final kinetic energies of protons, respectively.

III. RESULTS AND DISCUSSION

A. d-electron excitation in low-energy regime

The electronic energy loss of protons colliding with zinc atom in the low-energy range is displayed in Fig. 1(a). It can be seen from the figure that the electronic energy loss increases with the proton velocity. But the electronic energy loss reduces at 0.2 a.u. in model A, it continues to increase until the velocity is at 0.3 a.u., and it is proportional to the velocity in the range from 0.5 to 1.0 a.u. In model B, the electronic energy loss increases dramatically below 0.5 a.u., and it is proportional to the velocity from 0.6 to 1.0 a.u.

The electron energy levels of atomic zinc are discreted. When the transferred energy from the proton to the zinc atom exceeds the energy gap between the highest occupied atomic orbital and the lowest unoccupied atomic orbital of atomic zinc, the electrons in the highest occupied orbital will be excited to the lowest unoccupied one. When the transferred energy is lower than the energy gap, the electron excitation will be suppressed. In model A, there is not any growth in the electronic energy loss at 0.4 a.u., which is attributed to the threshold effect that results from the discretization nature of the atomic energy levels. However, since the contribution of charge transfer to the electronic energy loss is significant in the low-energy regime, the threshold effect caused by electron excitation is not fully demonstrated in electronic energy loss. In model B, the increase in electronic energy loss is suppressed at 0.5 a.u.

In order to further understand the relationship between the electronic energy loss and the number of excited electrons,

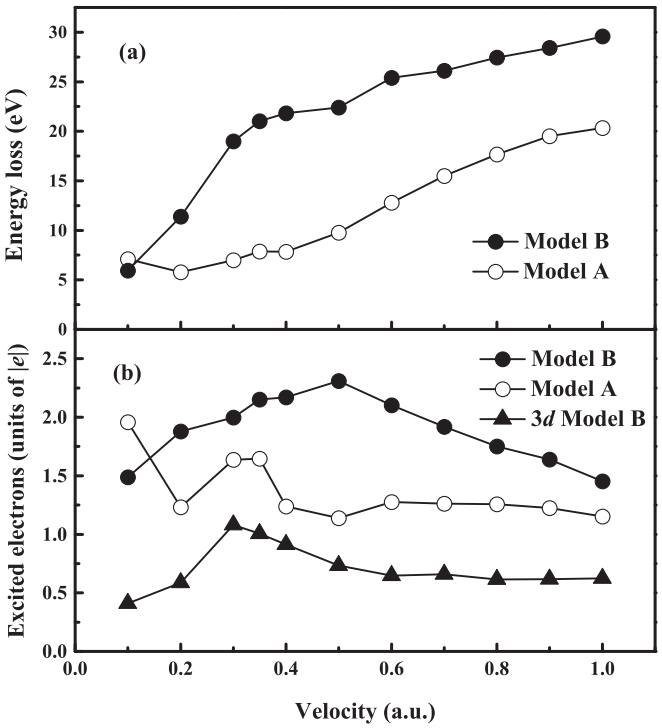

FIG. 1. The electronic energy loss (a) and the excited electrons (b) as a function of velocity. The impact parameter is 0.77 Å. Open and solid circles indicate results obtained from model A ($[\text{Ar}3d^{10}]4s^2$) and model B ($[\text{Ar}]3d^{10}4s^2$), respectively. Solid triangles in (b) represent the electrons excited only from $3d$ states in model B.

the number of excited electrons in both model A and B is obtained, as shown in Fig. 1(b). It can be seen that, except for 0.1 a.u., the total number of excited electrons in model B is larger than that in model A. Interestingly, when the velocity increases from 0.1 to 0.2 a.u., the total number of excited electrons decreases in model A, which is consistent with the behavior of the electronic energy loss. In model A, there are two electron excitation growth points at 0.30 and 0.35 a.u. It can be derived that the resonance excitation occurs at the two velocity points, at which the transferred energy is close to or equal to the threshold energy for $4s$ electrons excited to $4p$ and $5s$ states, respectively.

For a binary collision, the electronic excitation threshold can be calculated by [35]:

$$E_p \geqslant \frac{\mu^2}{4Mm_e}(E_k - E_{k_0})\left[1 + \frac{m_e}{\mu}\right]^2, \tag{6}$$

where the μ is the reduced mass of projectile-target system, E_p is the minimum kinetic energy of proton required for electron excitation, $E_k - E_{k_0}$ is energy absorbed by the electronic system of target atom, M is the projectile mass and m_e is the electronic mass. For the zinc atom in model A, the lowest transition is $4s \rightarrow 4p$, the energy gap as calculated between the ground $4s$ and $4p$ states is 4.80 eV. Therefore, the threshold velocity obtained from Eq. (6) for the electron excitation is at $v = 0.289$ a.u., which is in a good agreement with the velocity point at 0.30 a.u. For the case of $4s \rightarrow 5s$, with an

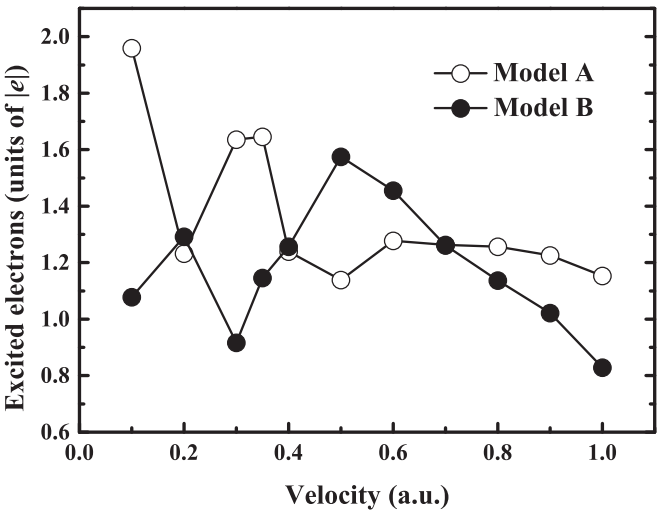

FIG. 2. The number of electrons excited from 4*s* state in model A ([Ar3d^{10}]4s^2) (open circles) and model B ([Ar]3d^{10}4s^2) (open triangles), respectively. The impact parameter is 0.77 Å. The lines are used only to guide the eye.

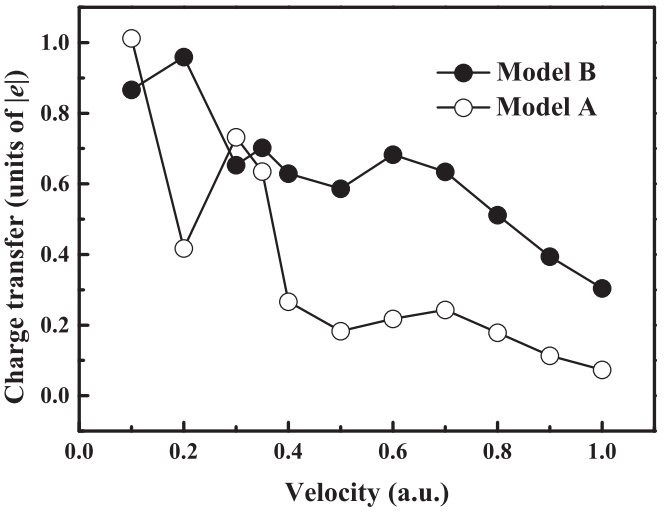

FIG. 4. The number of charges transferred to protons as a function of velocity. Open circles and solid circles represent results obtained from model A and model B, respectively.

excitation energy of 6.39 eV, the calculated threshold velocity is 0.334 a.u., which agrees well with the velocity of 0.35 a.u.

Because the transferred energy from the protons to the electronic subsystem of the zinc atom is not enough to excite the electrons at 0.1 a.u., the electronic energy loss here is caused by other channels, such as charge transfer. According to the formula, however, the calculated velocity threshold for 3*d* electrons excited to 4*p* states is 0.40 a.u. Since the 3*d* electrons can be excited to the 4*s* orbitals when 4*s* electrons are excited, so 3*d* electrons can be excited before the incident velocity reaches 0.4 a.u. In addition, according to the formula, the threshold velocity for 3*d* electrons excited to 4*s* state is at 0.27 a.u., but our results show that 3*d* electrons start to leave the orbitals when the velocity is 0.1 a.u., so the transition of *d* electrons is mediated by the charge transfer. As the velocity continues to increase, the *d* electron starts to be excited and the maximum number of excited 3*d* electron is emerged at 0.3 a.u. We considered that the rapid increase in the electronic energy loss below 0.5 a.u. is related to the simultaneous excitation of 4*s* and 3*d* electrons.

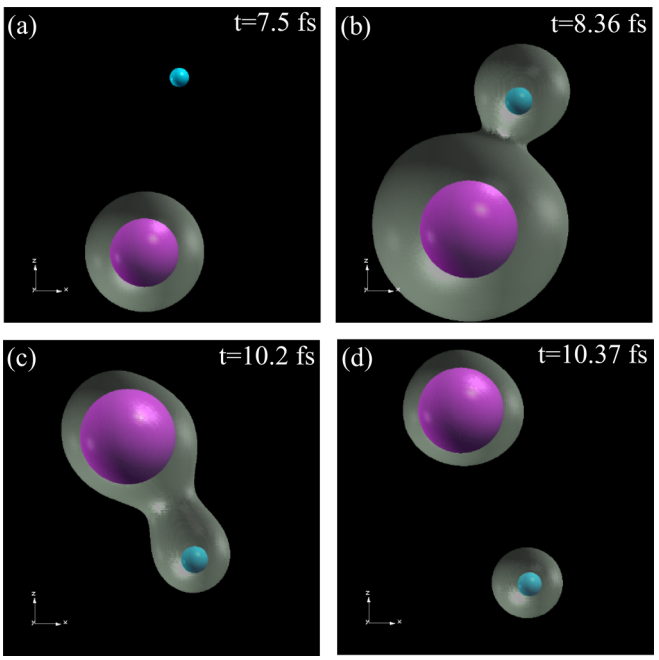

FIG. 3. Snapshots of the three-dimensional electron density of proton colliding with atomic zinc at 0.1 a.u. with $b = 0.77$ Å in model A. Panels (a), (b), (c) and (d) correspond to the moments at 7.5 fs, 8.36 fs, 10.2 fs, and 10.73 fs, respectively. The purple and blue balls represent Zn atom and proton, respectively. The electron density is shown with the gray region around the ball, and the isosurface value is set to be 0.2 $e/Å^3$.

In order to study the effects of the presence of 3*d* electrons on the excitation behavior of 4*s* electrons, the number of excited electrons from 4*s* state in both model A and B is shown in Fig. 2. The results show that the semicore electrons affect the excitation of 4*s* electrons, which is commonly known as the "shake-up" effect [21,36]. Our calculations show that the excitation of 4*s* electrons is suppressed above 0.7 a.u. in model B. By comparing the electronic energy losses between $b = 0.77$ Å and $b = 1.0$ Å in model B, we estimated that the contribution of *d* electron excitation to the electronic energy loss is about 60% in the velocities ranging from 0.5 to 1.0 a.u., ignoring the negligible change in the number of excited 4*s* electrons. At 0.1 a.u., the excitation of nearly two electrons in model A is thought to be caused by the charge transfer due to the long enough interaction time, but the number of excited electrons from 4*s* state is much lower in model B than in model A. As the velocity increases to 0.2 a.u., the effective contact time between the proton and the zinc atom decreases, so the number of electrons captured by the proton decreases rapidly in model A, meanwhile the electronic energy loss is also reduced. The electronic energy loss is dominated by charge transfer with velocities of less than 0.2 a.u. in model A. It was reported that the charge transfer dominates the energy loss in the collisions between

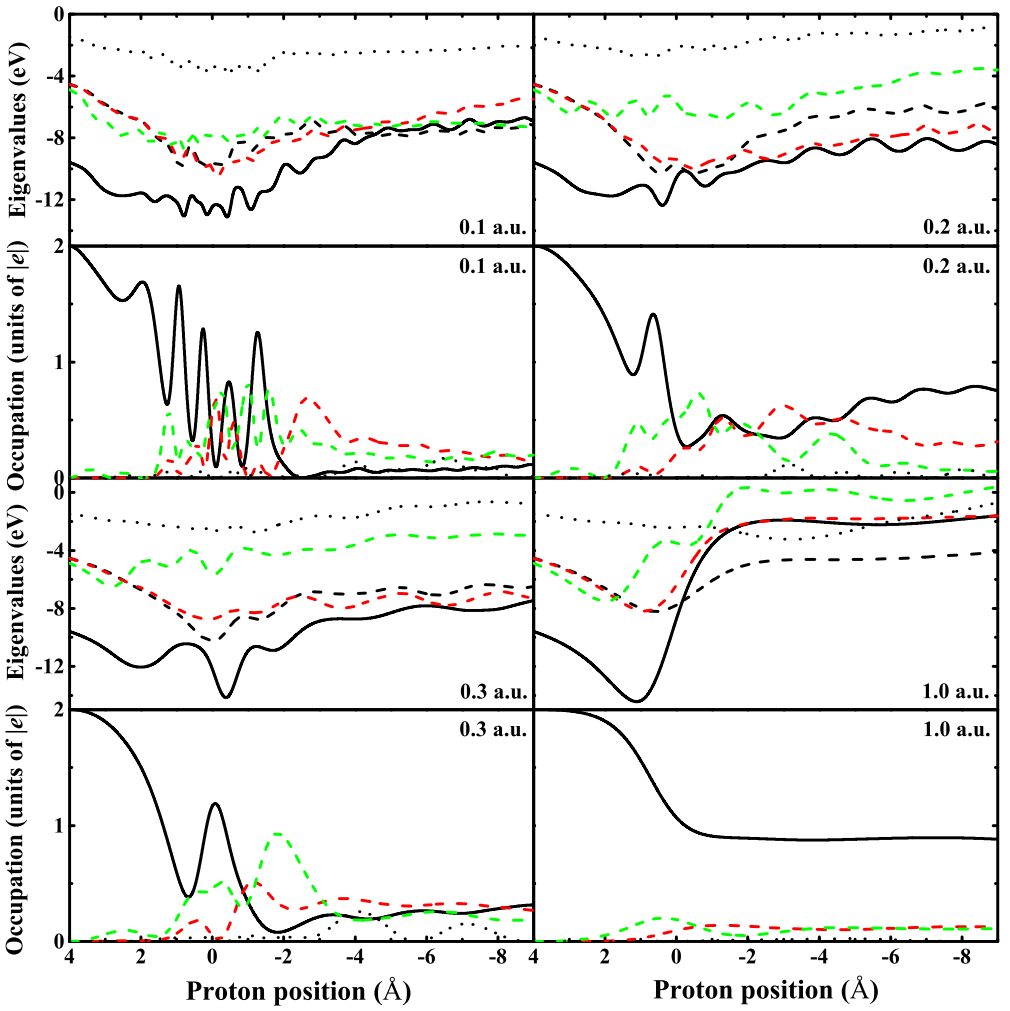

FIG. 5. The energy eigenvalues and electron occupations of 4s, 4p, and 5s states of zinc atom as a function of proton position along z axis in model A ([Ar3d^{10}]4s^2). The solid lines refer to 4s state, the dashed lines refer to 4p states, and the dotted lines refer to 5s states. Different colors represent different degenerate states of 4p.

low-energy protons and zinc atoms, the scattering angle of the protons has a great influence on the charge transfer behavior [35]. We notice that the resonance excitation disappears when 3d electrons are activated (see Fig. 2). The electrons in the bound states are greatly excited as the velocity increasing.

The charge transfer processes between the proton and the zinc atom are illustrated by the charge density evolution of the ion-atom system with $b = 0.77$ Å at 0.1 a.u. in model A, as presented in Fig. 3. It can be seen that, the proton captures a certain number of electrons as it approaches the zinc atom, then the electron-carrying proton collides with the zinc atom, and the charges of the ion-atom system combine, eventually redistributing electrons as they separate. The evolution of the charge density suggests the formation of a quasimolecule by the ion-atom system in the collision process at 0.1 a.u, which provides a channel to raise electrons from bound state to unoccupied state of the proton [37].

The number of electrons captured by protons after the collision is shown in Fig. 4. Overall, the number of charge transfer decreases as the velocity increases, and it is greater in model B than that in model A except for 0.1 and 0.3 a.u. It is noticed that the charge transfer shows the same behavior as the electron excitation in model A. However, the number of charge transfer is significantly less than the number of excited electrons in both model A and B. The reason is that the excited electrons are partly captured by protons and partly scattered into vacuum space. With increasing the velocity, the electrons in the bound state are excited to the high level state in large quantities, and the electrons can be easily captured by the protons. As the velocity continues to increase, the target electrons do not have enough time to react to the protons, so the amount of charge transfer gradually decreases.

B. Energy eigenvalues and electron occupations

In order to clarify the change of electronic energy loss and electron excitation at some velocities, the evolution of the energy eigenvalues and electron occupations during the collisions are examined in detailed. The eigenvalues and occupation at 0.1, 0.2, 0.3, and 1.0 a.u. in model A are shown in Fig. 5. At 0.1 a.u., we can see that the energy levels of 4s and 4p states overlap after the collision, and the 4s electrons are almost all left. The transferred energy is not enough to completely excite the 4s state to the 4p state. It

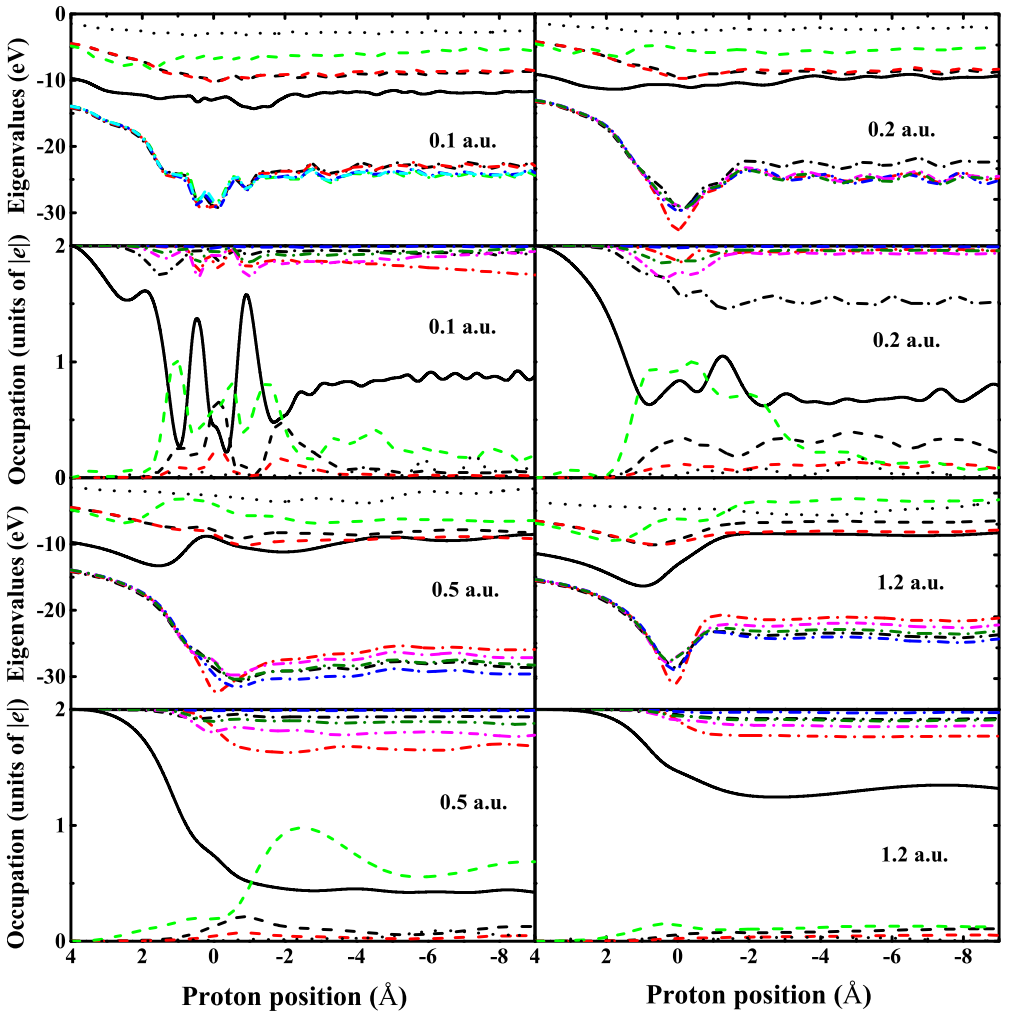

FIG. 6. The energy eigenvalues and electron occupations of 3*d*, 4*s*, 4*p*, and 5*s* states of zinc atom as a function of proton position along *z* axis in model B ([Ar]$3d^{10}4s^2$). The dash-dotted lines refer to 3*d* states, the solid lines refer to 4*s* state, the dashed lines refer to 4*p* states, and the dotted lines refer to 5*s* states. Different colors of the same line distinguish different degenerate orbitals.

can be seen from the evolution of the number of electron occupations, about 1.0 electron is captured by the proton, and much of the rest 4*s* electrons are excited into the vacuum. At 0.2 a.u., 4*s* state is lifted up to the lowest 4*p* state, the number of 4*s* electrons increases again at −3 Å after the collisions, which is caused by the direct Coulomb interaction between the proton and the zinc atom. Because the transferred energy is not enough to excite 4*s* electrons, the electrons that are attracted to the proton go back to the 4*s* state. It is noted that there are a few excited electrons left in the 4*p* states. At 0.3 a.u., a significant peak is displayed in the occupation of one of the 4*p* states near the −2 Å indicating that electrons are once transited to the 4*p* state during the dynamic process of the collision, which convinces that the resonance excitation of the 4*s* electrons to the 4*p* states. The velocity corresponding to the maximum number of excited electrons is different from the velocity corresponding to the maximum electronic energy loss. It is noticed that in model A, the electronic energy loss reaches its maximum at velocity of 1.0 a.u., at which the 4*s* state is completely lifted to the 5*s* state after the collision. Of all the velocities, the 4*s* state is excited to the highest energy level at 1.0 a.u. Here, since 4*s* state is completely lifted to 5*s* state, all the electrons located at 4*s* state have the same energy of 5*s* state. That is, besides part of electrons are excited to higher energy states, all the remaining 4*s* electrons are excited to 5*s* state.

Figure 6 shows the time evolution of the energy eigenvalues and electron occupation at some velocity points in model B. At 0.1 a.u., the electrostatic interaction between the proton and the zinc atom simulates not only the 4*s* electrons, but also the 3*d* electrons. At 0.2 a.u., 3*d* and 4*s* electrons are left from the occupied states, which is probably due to the charge transfer. At 0.5 a.u., the 4*s* state is lifted up to the energy level of the 4*p* states, so the 4*s* electrons have the same energy with the 4*p* electrons, even though there are still some electrons in the 4*s* state, we can consider that the other 4*s* electrons are excited to 4*p* states. As the 4*s* state is completely lifted up to the 4*p* state, the 3*d* electrons can only be excited to 4*p* states. According to Eq. (6), the threshold velocity required to excite 3*d* electrons to 4*p* states is 0.58 a.u., that is the reason why the electronic energy loss does not increase significantly at 0.5 a.u. in model B. It is important to note that

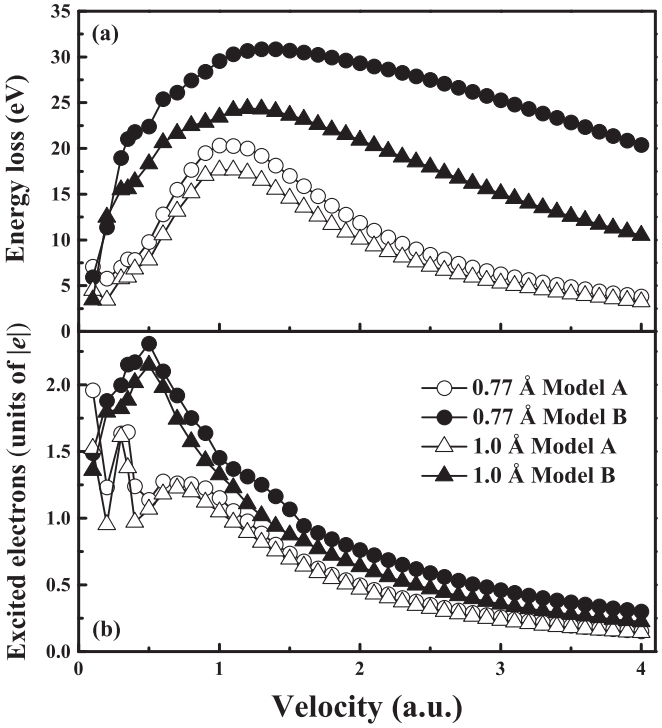

FIG. 7. The electronic energy loss (a) and the number of excited electrons (b) as a function of velocity. Open circles and solid circles indicate the electronic energy loss with $b = 0.77$ Å in model A ([Ar3d^{10}]4s^2) and B ([Ar]3d^{10}4s^2), respectively. Open triangles and solid triangles represent the electronic energy loss in the case of $b = 1.0$ Å.

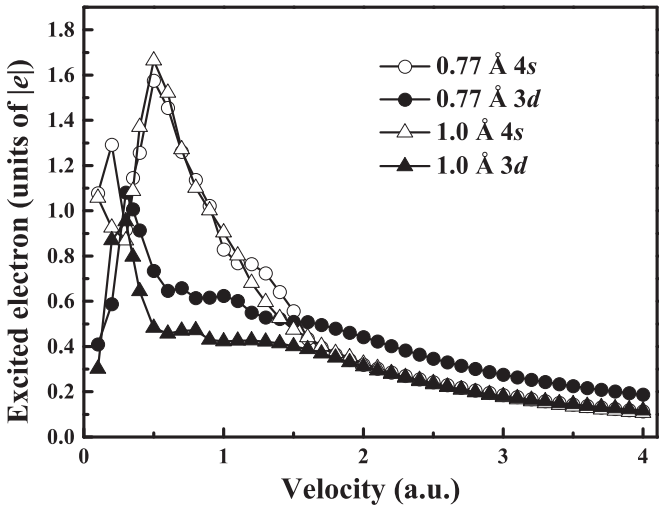

FIG. 8. The number of electrons excited from 3d (solid symbols) and 4s (open symbols) states in model B ([Ar]3d^{10}4s^2), respectively. Circles represent the results with $b = 0.77$ Å, and triangles represent the results with $b = 1.0$ Å.

due to the significant contribution of the charge transfer to the electronic energy loss in the low-energy regime, not all of the electrons are excited strictly in the order from lower energy levels to higher ones, there is a large part of electrons can be captured directly by the protons rather than from the level gradually.

The electronic energy loss reaches the maximum value at 1.2 a.u. in model B. It can be seen from the figure that, the 4s state is completely lifted up to the 4p states. This result again shows that the existence of d electrons inhibits the highest energy state to which 4s electrons can be excited. Taking all the data together, the effect of d electrons on the electronic energy loss of atomic zinc is significant in the low-velocity range. As for the number of excited electrons, the contribution of 4s electrons still dominates. Except for the maximum value of d-electron excitation at 0.3 a.u., see Fig. 1(b), the number of excited d electrons is less than half of the total number of excited electrons.

C. Effect of impact parameter on d-electron excitation

The effects of impact parameter on the energy loss and d electron excitation are examined in a wide range of velocities, as shown in Fig. 7. It can be seen from Fig. 7(a) that, the excitation of 3d electrons contributes significantly to the electronic energy loss in the entire energy range studied. When d electrons are frozen (in model A), the electronic energy loss is insensitive to the impact parameter. However, the electronic energy loss shows a strong dependence on the impact parameter when the d electrons are activated (in model B). For $b = 1.0$ Å, the contribution of d electron excitation to the energy loss is only about 9 eV, which comprises about 60% of the total energy loss in the velocity range from 2.0 a.u. to 4.0 a.u. However, for $b = 0.77$ Å, the excitation of d electrons increases the electronic energy loss by about 18 eV, which accounts for about 80% of the total energy loss in the same energy range. So the contribution of d electron excitation to the electronic energy loss is getting increased as the impact parameter decreasing. The energy loss behavior is consistent with that of the number of excited electrons, as shown in Fig. 7(b). As the impact parameter varies from $b = 1.0$ Å to $b = 0.77$ Å, the total number of excited electrons is almost the same in model A, but it is increased by 25% in model B.

To further determine the contribution of 3d electrons excitation to the electronic energy loss, the number of electrons excited from 4s and 3d states are separated from the total number of excited electrons in model B, as shown in Fig. 8. It can be seen from the figure that, as the impact parameter increases from 0.77 Å to 1.0 Å, the number of electrons excited from 4s state remains almost the same, but that from 3d states decreases by about 33% from 2.0 a.u. to 4.0 a.u. In the case of $b = 0.77$ Å, the number of excited 3d electrons exceeds that of 4s electrons when the velocity is greater than 1.5 a.u. Finally, we compared the electronic energy levels during the collision between $b = 0.77$ Å and 1.0 Å in model B, here we only present the results of 4.0 a.u. in Fig. 9. The average energy eigenvalue of 3d electrons after the collision are -12.4 eV and -12.357 eV for $b = 1.0$ Å and 0.77 Å, respectively. Hence, the effect of the final excited energy level on the energy loss is negligible. So, we can determine that the gap in the electronic energy loss between $b = 0.77$ Å and 1.0 Å is entirely ascribed to the excitation of 3d electrons.

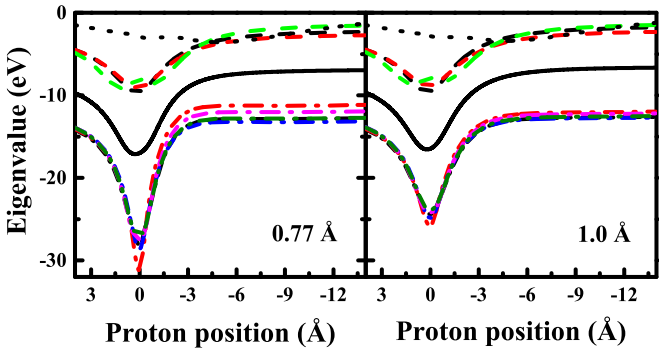

FIG. 9. The eigenvalues of exited states of zinc atom as a function of proton position with $b = 0.77$ Å (left) and $b = 1.0$ Å (right) at 4.0 a.u. in model B ([Ar]$3d^{10}4s^2$), respectively. The dash-dotted lines refer to 3*d* states, the solid lines refer to 4*s* state, the dashed lines refer to 4*p* states, and the dotted lines refer to 5*s* state. Different colors of the same line distinguish different degenerate orbitals.

D. Stopping cross section

The results of SCS of protons colliding with atomic zinc is shown in Fig. 10, as well as the other theoretical results and the experimental data [38,39] are also shown for comparison. The SCSs obtained from model A are in good agreement with the experimental data from Ref. [38] and SRIM data [40] to 0.4 a.u., which means that the excitation of 4*s* electrons dominates the energy loss of bulk Zn in this energy range. As the velocity increases, our calculated results increase rapidly and get close to the measured data obtained from gas-state zinc target. Noting that our data agree well with the experimental measurements [39] of the gas target around 1.0 a.u., this is because the charge transfer, electron excitation and ionization effects all contribute to the electronic energy loss in this velocity range. Moreover, in our calculations, the electronic SCS is calculated by considering the contributions of all collision events with energy loss, which is similar to the situation of protons colliding with gas-state target in which all possible impact parameters may be sampled. Our results displayed that the excitation of 4*s* electrons is sufficient to describe the electronic SCS of gas-state zinc target in the intermediate velocity regime.

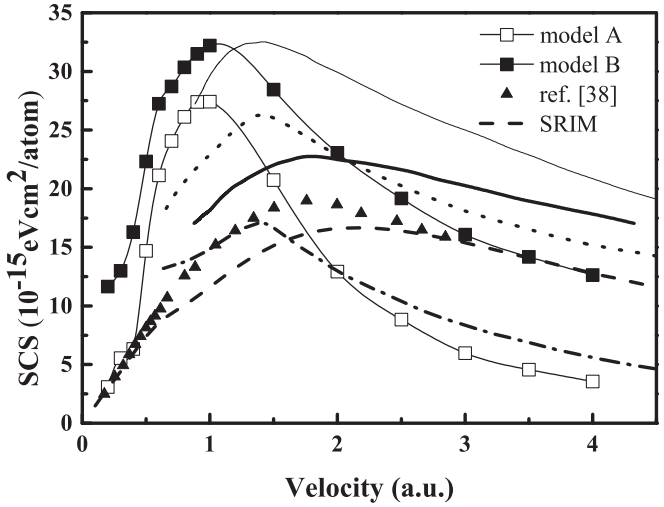

FIG. 10. Stopping cross section for proton colliding with atomic zinc as a function of the velocity. Open and solid squares indicate the results obtained from models A ([Ar3d^{10}]$4s^2$) and B ([Ar]$3d^{10}4s^2$), respectively. The dotted and dash-dotted lines indicate the contributions of 3*d*+4*s* and 4*s* electron excitation to the stopping cross section of zinc [39], respectively. The thick and thin lines indicate the experimental data of solid and gas phase zinc [39], respectively. The triangles indicate the experimental measurements of bulk zinc from Ref. [38]. The dashed line indicates the SRIM data.

In the high-velocity regime, the SCSs obtained from model B are in good agreement with the experimental data and SRIM data, which supports that the contributions from *d*-electron excitation to the electronic energy loss is becoming dominant as the incident energy increasing. The 4*s* electron contribution reported in Ref. [39] is slightly higher than the result obtained from model A when the velocity is beyond 2.0 a.u. It is calculated that the proportion of 3*d*-electron excitation to the SCS exceeds 50% when the velocity exceeds 2.0 a.u in the present study, while it exceeds 55% which results in the SCSs are higher than the measured data by 10% in Ref. [39]. However, our results are still lower than those obtained from the gas-state target, which suggests that more core electrons may be considered to match the experimental data of gas phase target in the high-velocity regime.

IV. CONCLUSIONS

In the present work, we studied the behavior of 3*d* electrons excitation of atomic zinc triggered by energetic protons collision within first-principles molecular dynamics simulations based on real-time time-dependent density-functional theory. In the low-energy regime, the electronic energy loss displays a threshold effect due to the discrete electronic energy levels of the zinc atom. The energy loss is increased at the threshold velocities due to the resonance excitation, in which the transferred energy from the protons to the target atom is equal to the energy gap between the atomic energy levels. Moreover, the presence of 3*d* electrons suppresses the excitation of 4*s* electrons when the incident velocity is beyond 0.7 a.u., and it also restricts the highest energy level to which 4*s* electrons can be excited. On the other hand, the charge transfer has a great influence on the electronic energy loss at 0.1 a.u. In the low-energy regime, it is enough to consider the excitation of 4*s* electrons for describing the electronic stopping cross section of protons colliding with atomic zinc.

The effects of impact parameter on *d* electron excitation are investigated in this study. Our results show that *d* electron excitation is dependent on the impact parameter in the collision. The number of excited *d* electrons is increased as the impact parameter decreasing, leading to the electronic energy loss is greatly enhanced. The contribution of *d* electron excitation to the electronic energy loss is becoming dominant with the increase of incident velocity. The stopping cross sections are found to be consistent with measured data when the *d* electron excitations are activated in the high-energy regime, and the proportion of *d* electron excitation to the stopping cross section exceeds 50% when the velocity is beyond 2.0 a.u. So, the contribution of *d* electrons excitation to the energy loss should be taken into account in the high-energy region.

ACKNOWLEDGMENTS

This work is supported by the National Natural Science Foundation of China under Grants No. 11975119, No. 11505092, and No. 11774030; the Natural Science Foundation of Hunan Province, China (Grant No. 2017JJ3266); and the Research Foundation of Education Bureau of Hunan Province, China (Grant No. 18B261). This work is also partially supported by the PhD Start-up Foundation of University of South China (USC) under Project No. 2014XQD06 and the Construct Program of the Key Discipline in Hunan Province.

[1] V. G. Kapinos and D. J. Bacon, Phys. Rev. B **50**, 13194 (1994).

[2] P. Patel, A. Mackinnon, M. Key, T. Cowan, M. Foord, M. Allen, D. Price, H. Ruhl, P. Springer, and R. Stephens, Phys. Rev. Lett. **91**, 125004 (2003).

[3] R. H. Ritchie, Phys. Rev. **114**, 644 (1959).

[4] P. M. Echenique, R. M. Nieminen, J. C. Ashley, and R. H. Ritchie, Phys. Rev. A **33**, 897 (1986)

[5] J. F. Ziegler, J. Appl. Phys. **85**, 1249 (1999).

[6] S. N. Markin, D. Primetzhofer, and P. Bauer, Phys. Rev. Lett. **103**, 113201 (2009).

[7] L. N. Serkovic Loli, E. A. Sánchez, O. Grizzi, and N. R. Arista, Phys. Rev. A **81**, 022902 (2010).

[8] E. Fermi and E. Teller, Phys. Rev. **72**, 399 (1947).

[9] J. M. Pruneda, D. Sánchez-Portal, A. Arnau, J. I. Juaristi, and E. Artacho, Phys. Rev. Lett. **99**, 235501 (2007).

[10] A. A. Correa, J. Kohanoff, E. Artacho, D. Sánchez-Portal, and A. Caro, Phys. Rev. Lett. **108**, 213201 (2012)

[11] A. Schleife, Y. Kanai, and A. A. Correa, Phys. Rev. B **91**, 014306 (2015).

[12] C.-K. Li, F. Wang, B. Liao, X.-P. OuYang, and F.-S. Zhang, Phys. Rev. B **96**, 094301 (2017).

[13] E. E. Quashie, B. C. Saha, and A. A. Correa, Phys. Rev. B **94**, 155403 (2016).

[14] A. Lim, W. M. C. Foulkes, A. P. Horsfield, D. R. Mason, A. Schleife, E. W. Draeger, and A. A. Correa, Phys. Rev. Lett. **116**, 043201 (2016).

[15] E. E. Quashie, B. C. Saha, X. Andrade, and A. A. Correa, Phys. Rev. A **95**, 042517 (2017).

[16] D. Goebl, D. Roth, and P. Bauer, Phys. Rev. A **87**, 062903 (2013).

[17] S. N. Markin, D. Primetzhofer, M. Spitz, and P. Bauer, Phys. Rev. B **80**, 205105 (2009).

[18] E. D. Cantero, G. H. Lantschner, J. C. Eckardt, and N. R. Arista, Phys. Rev. A **80**, 032904 (2009).

[19] A. A. Shukri, F. Bruneval, and L. Reining, Phys. Rev. B **93**, 035128 (2016).

[20] A. Ojanperä, A. V. Krasheninnikov, and M. Puska, Phys. Rev. B **89**, 035120 (2014).

[21] Y. Yao, D. C. Yost, and Y. Kanai, Phys. Rev. Lett. **123**, 066401 (2019).

[22] R. Ullah, E. Artacho, and A. A. Correa, Phys. Rev. Lett. **121**, 116401 (2018).

[23] D. Goebl, W. Roessler, D. Roth, and P. Bauer, Phys. Rev. A **90**, 042706 (2014).

[24] A. Castro, M. Isla, J. I. Martínez, and J. A. Alonso, Chem. Phys. **399**, 130 (2012).

[25] G. Avendaño-Franco, B. Piraux, M. Grüning, and X. Gonze, Theor. Chem. Acc. **131**, 1289 (2012).

[26] F. Wang, X. C. Xu, X. H. Hong, J. Wang, and B. C. Gou, Phys. Lett. A **375**, 3290 (2011).

[27] X. Andrade, D. A. Strubbe, U. De Giovannini, A. H. Larsen, M. J. T. Oliveira, J. Alberdi-Rodriguez, A. Varas, I. Theophilou, N. Helbig, M. Verstraete, L. Stella, F. Nogueira, A. Aspuru-Guzik, A. Castro, M. A. L. Marques, and A. Rubio, Phys. Chem. Chem. Phys. **17**, 31371 (2015).

[28] X. Andrade, J. Alberdi-Rodriguez, D. A. Strubbe, M. J. T. Oliveira, F. Nogueira, A. Castro, J. Muguerza, A. Arruabarrena, S. G. Louie, A. Aspuru-Guzik, A. Rubio, and M. A. L. Marques, J. Phys.: Condens. Matter **24**, 233202 (2012).

[29] X. Andrade, A. Castro, D. Zueco, J. L. Alonso, P. Echenique, F. Falceto, and A. Rubio, J. Chem. Theory Comput. **5**, 728 (2009).

[30] J. P. Perdew and Y. Wang, Phys. Rev. B **45**, 13244 (1992).

[31] A. Castro, M. A. L. Marques, and A. Rubio, J. Chem. Phys. **121**, 3425 (2004).

[32] N. Troullier and J. L. Martins, Phys. Rev. B **43**, 1993 (1991).

[33] J. G. Muga, J. P. Palao, B. Navarro, and I. L. Egusquiza, Phys. Rep. **395**, 357 (2004).

[34] T. Otobe, M. Yamagiwa, J.-I. Iwata, K. Yabana, T. Nakatsukasa, and G. F. Bertsch, Phys. Rev. B **77**, 165104 (2008).

[35] R. Cabrera-Trujillo, J. R. Sabin, Y. Öhrn, and E. Deumens, Phys. Rev. Lett. **84**, 5300 (2000).

[36] P. Persson, S. Lunell, A. Szöke, B. Ziaja, and J. Hajdu, Protein Sci. **10**, 2480 (2001).

[37] K. Eder, D. Semrad, P. Bauer, R. Golser, P. Maier-Komor, F. Aumayr, M. Peñalba, A. Arnau, J. M. Ugalde, and P. M. Echenique, Phys. Rev. Lett. **79**, 4112 (1997).

[38] G. Martínez-Tamayo, J. C. Eckardt, G. H. Lantschner, and N. R. Arista, Phys. Rev. A **54**, 3131 (1996).

[39] P. Bauer, F. Kastner, A. Arnau, A. Salin, P. D. Fainstein, V. H. Ponce, and P. M. Echenique, Phys. Rev. Lett. **69**, 1137 (1992).

[40] J. F. Ziegler and J. P. Biersack, The Stopping and Range of Ions in Matter, http://www.srim.org./.